

A simple monatomic ideal glass former: the glass transition by a first-order phase transition above the melting point

Måns Elenius¹, Tomas Opperstrup^{1,3} and Mikhail Dzugutov²

¹*Department of Numerical Analysis and* ²*Department of Materials Science and Engineering, Royal Institute of Technology, 100 44 Stockholm, Sweden*

³*Lawrence Livermore National Laboratory, Livermore, California 94551, USA*

Abstract

A liquid can form under cooling a glassy state either as a result of a continuous slowing down or by a first order polyamorphous phase transition. The second scenario has so far always been observed below the melting point where it interfered with crystalline nucleation. We report the first observation of the liquid-glass transition by a first order phase transition above the melting point. The observation was made in a molecular dynamics simulation of a one-component system with a model metallic pair potential. This is also the first observation of a simple monatomic ideal glass former – a liquid that avoids crystallization at any cooling rate. Besides its conceptual importance, this result indicates a possibility of existence of metallic ideal glass formers.

Periodic phases are commonly thought to be thermodynamically favoured at sufficiently low temperatures by all substances. The relaxation time of a liquid in its domain of thermodynamic stability, above T_m , is usually much smaller than the value of $10^2 s$ that defines the glass-transition temperature T_g (1). Therefore, a fundamental problem of the glass science is to avoid the interference of crystalline nucleation when cooling a liquid within the metastability domain $T_g < T < T_m$. The ideal glass former (2) is defined by the condition $T_g > T_m$ which excludes the possibility of its crystallisation upon cooling. This class of glass formers has so far been found to include atactic polymers (3) and some aqueous solutions of electrolytes (4). A simple monatomic liquid that does not crystallize upon cooling has so far never been found. The question of its existence is intellectually challenging, conceptually important and also of a significant technological interest, particularly for the area of metallic glasses.

A straightforward strategy for reducing T_m relative to T_g is to frustrate the crystallization by structural complexity. In non-polymeric systems, this can be achieved by tuning anisotropic interaction (5), by a judiciously designed pair potential (6), or by composing multicomponent eutectic mixtures (4, 7, 8). Crystallization of a liquid upon cooling can also be precluded by a direct first order polyamorphous transition to a glassy state. Such a transition, however, has so far always been observed below T_m (9), where the presence of a liquid-liquid spinodal significantly enhances crystalline nucleation (10, 11). Moreover, a liquid-liquid transition has never been observed in a monatomic system upon cooling above T_m (12). The Jagla soft-core pair potential produces two stable liquid phases. However, because of a significant difference in densities, the transition between these phases has only been found under compression and not upon cooling (13, 14).

Here, we report a simple monatomic liquid that remains stable with respect to crystallization upon cooling but performs a first order polyamorphous phase transition to a phase with a mesoscopic-range order and the rate of structural relaxation characteristic of the glassy state. Thus, the liquid, avoiding crystallization at any cooling rate, is an ideal glass former.

The liquid was explored in a molecular dynamics simulation. It used a model pair potential (15) (named Z2 in that reference) designed to imitate effective interionic interaction potentials in liquid metals with characteristic Friedel oscillations (16, 17). The simulation was performed using a system of $N = 128000$ particles. A smaller system of $N = 3456$ particles has also

been explored in order to test the size-dependence of the observed phenomenon. We note that the main repulsive part of the pair potential used in this model closely approximates that of the Lennard-Jones potential. Interpreting the latter as a model potential of argon (18), the units of length and time used in this simulation correspond to 0.34 nm and 2.16 ps, respectively. All other quantities reported here are expressed in these reduced units.

We cooled the large system from the high-temperature liquid state isochorically at the number density $\rho = 0.85$ by changing the temperature T in a stepwise manner, with a comprehensive equilibration at each temperature step. The results presented in Fig. 1a show a discontinuous enthalpy drop on cooling at $T = 0.72$. Reheating of the lower temperature results in a pronounced hysteresis, an unambiguous signature of a first order phase transition.

Fig. 1b shows the structure factor $S(Q)$ for the two phases. The similarity of the two curves indicates that we observe a first order transition between two similarly structured liquid phases, to be referred to as the high-temperature liquid (HTL) and the low temperature liquid (LTL). The split in second peak of $S(Q)$ featured by both liquid phases indicates a strong tetrahedral local order (19).

We now explore the transition domain in the $P - \rho$ phase diagram at constant T . Fig. 1c shows the LTL isotherms produced by heating, compression and/or expansion of the original states of that phase obtained under isochoric cooling at $\rho = 0.85$. All the data were produced after comprehensive equilibration. The regions of infinite compressibility indicate the existence of a domain of spinodal instability interposed between the two liquid phases. We find that the phase behaviour of the small system (N=3456) reproduces the behavior of the large system along the $T = 0.75$ isotherm. Expectedly, the small system size results in shrinking of the instability domain.

Infinite compressibility in the spinodal domain manifests in diverging long-wavelength limit of $S(Q)$, a measure of the density fluctuations on the system-size scale. In a macroscopic system, $S(0)$ is related to the isothermal compressibility χ_T by the compressibility equation: $S(0) = \rho k_B T \chi_T$ (18). Fig. 1d shows the density-dependence of the small- Q behaviour of $S(Q)$ along the $T = 0.78$ isotherm. A trend for divergence of the small- Q limit of $S(Q)$ is clearly visible at the densities where the spinodal instability was detected from the respective isotherm in Fig. 1c. Note that there is no divergence in the small- Q limit of $S(Q)$ for the LTL

in Fig. 1b, indicating that at $T = 0.68, \rho = 0.85$ it is below the spinodal domain.

Fig. 2 presents a real-space picture of the spinodal decomposition of a system of 128000 particles along the $T = 0.78$ isotherm. The plots depict cross-sections of the coarse-grained spatial distribution of energy. For $\rho = 0.84$ representing the HTL phase, the energy is distributed uniformly. At $\rho = 0.87$, precipitation of the LTL phase appears as distinct large-scale low-energy domains. Upon further isothermal compression, the LTL domains grow and eventually percolate as the system leaves the spinodal domain. This is indicated by the reduction of the isothermal compressibility in the isotherms as shown in Fig. 1d. Respectively, the HTL domains shrink and become disconnected, arguably giving rise to the low- Q pre-peak of the respective $S(Q)$ visible in Fig. 1d. This is consistent with the conjecture (20) that a LTL phase is intrinsically heterogeneous.

In order to understand the nature of the observed phase transition, we analysed details of the structural transformation between the two phases. To remove thermally induced fluctuations, the investigated liquid configurations were subjected to the steepest descent energy minimisation. In the structure analysis we used an earlier developed method of identifying the tetrahedral local order (6). All the particles comprising the first peak of the radial distribution function $g(r)$ were assumed to be the nearest neighbours. The narrow and sharp shape of the peak renders this definition of neighbours unambiguous.

We found that the HTL-LTL transition, while sustaining a strong tetrahedral local order, reduces the number of icosahedra by about 30%. This paradoxical observation can be understood by inspecting a characteristic cluster found in a low-temperature domain of the LTL in Fig. 2. The cluster, shown in Fig. 3a, can be described as a 5-fold tetrahelical configuration composed of axially stacked pentagonal bipyramides. The latter's pentagonal symmetry, however, is broken by a linear strain of non-tetrahedral defects that involves two adjacent helical lines of atoms, as shown in Fig 3b. The creation of such a defect reduces the energy by removing frustration inherent to the 5-fold packing of tetrahedra. Moreover, these defects facilitate aggregation of the tetrahelical clusters into an extended tetrahedral network. Fig. 3c shows two clusters which share a line of helically stacked 4-fold defects as depicted in Fig. 3d. In this way, extended tetrahedral configurations, apparently incompatible with periodic order, form under cooling a network that accounts for the observed immense viscosity of the LTL. Their

inability to uniformly fill the space renders the LTL intrinsically heterogeneous.

We now analyse the LTL dynamics at $\rho = 0.85$. The diffusivity plot in Fig. 4a, doesn't significantly change upon the transition, which is in contrast to the more than 2 orders of magnitude diffusivity drop observed at the glass transition in silicon (9). This can be attributed to the LTL heterogeneity demonstrated in Fig. 2, with possibly high diffusivity within the high-energy fluid domains. The temperature variation of the LTL diffusivity is perfectly exponential, indicating that the HTL-LTL transition results in a fragile-to strong crossover (9, 21). We also found the LTL diffusivity to be independent of the system size, which allowed us to use the small system to explore the low- T diffusion within affordable computer time.

The structural relaxation is controlled by the slowest-dissipating component of the intermediate scattering function $F(Q, t)$ (see Methods) within the structurally relevant range of Q . Estimating the Q -dependent relaxation time of $F(Q, t)$ in a liquid (18) as $\tau(Q) = S(Q)/Q^2$, we expect the small- Q prepeak of $S(Q)$ observed in Fig. 1b to be the slowest dissipating structural feature of the LTL phase. This conclusion is confirmed in the inset of Fig. 4b. The main panel of Fig. 4b shows the time variation of $F(Q_{pp}, t)$, Q_{pp} being the position of the prepeak, for $T = 0.65$ and $T = 0.6$. For both temperatures, the relaxation times clearly exceed by several orders of magnitude the time interval shown in the plot which, in terms of argon interpretation of the reduced units of time, corresponds to $0.65 \cdot 10^{-4}$ s. This makes it possible to conclude that the LTL is a structurally arrested glassy state.

The observed non-dissipation of $S(Q_{pp})$ implies that the spatial distribution of the low-energy clusters in the LTL that was concluded to give rise to the prepeak gets frozen below the spinodal domain. To support this conclusion, we present in Figs. 4c and 4d the evolution of the coarse-grained potential energy distribution in the LTL at $T = 0.65$ and $T = 0.60$, respectively. For each, T the time interval separating the plots corresponds to that spanned by the respective $F(Q_{pp}, t)$ shown in Fig. 4b. The apparent time invariance of the distribution indicates that the tetrahedrally ordered low-energy clusters like those shown in Fig. 3 form a percolating network which remains topologically unchanged on the explored time scale. Fig. 4e shows a cluster composed of face-sharing tetrahedra discerned within a low-energy domain at $T = 0.65$. The percolation is reminiscent of gelation in colloids forming a percolating network of linear clusters composed of tetrahedra (22). A similar percolation transition was

observed in the present system at low densities (23). A glass transition by percolation was also found in ideal polymeric glass-formers (3).

We note that the extended range of structural ordering within the tetrahedral clusters of the LTL phase gives rise to the anomalously high main peak of $S(Q)$, shown in Fig. 1b. This structural peculiarity, unusual for simple liquids, can be compared with the structure of mesophases, e.g. those formed by proteins (24). Moreover, the apparent structural heterogeneity of the LTL phase, and the relatively high diffusivity distinguish it from the typical inorganic glasses forming continuous tetrahedral networks. A feasible conjecture is that these distinctions of the present glass may possibly render it ductile and capable of self-repair, in contrast to the well-known brittleness of the inorganic glasses. This possibility is of significant technological interest, and deserves further investigation.

In summary, we presented a simple one-component system with a metal-like pair potential that behaves as an ideal glass former. Under cooling, the system performs a polyamorphous first order phase transition from a stable liquid phase to a glassy phase which precludes any possibility of crystallization. The prototypical metallic nature of the model suggests a possible new strategy for designing bulk metallic glass formers, distinct from the currently popular idea of frustrating crystallization by eutectically mixing a number of atomic species with strong mismatch in size (8). As a potentially relevant observation, we mention a strong-fragile transition found in a bulk metallic glass-forming alloy (25).

Based on these results, a possible strategy in the search for an ideal glass former in metallic systems may be suggested. The form of the pair potential we used (15) is ubiquitous in interionic effective potentials in metallic liquids (16). It incorporates the Friedel oscillations which are controlled by the electron density (17) and can therefore be regulated by modifying the composition of a metallic alloy. This way of tuning the interionic potentials in a real metallic liquid can be used to approximate the potential exploited in this study.

References

- [1] P. G. Debenedetti, F. Stillinger, *Nature* **410**, 259 (2001).
- [2] C. A. Angell, *J. Non-Cryst. Solids* **354**, 4703 (2008)
- [3] J.K. Kruger, K.-P. Bohn, R. Jimenez, and J. Schreiber, *Colloid Polym. Sci.*, **274**, 490 (1996)
- [4] E. J. Sare, and C. A. Angell, *Journ. of Sol. Chem.*, **2**, 53 (1973)
- [5] V. Molinero, S. Sastry, and C. A. Angell, *Phys. Rev. Lett.* **97**, 075701 (2006)
- [6] M. Dzugutov, S. Simdyankin, and F. Zetterling, *Phys. rev. Lett.* **89**, 195701 (2002)
- [7] W.-L. Johnson, *Mat. Res. Bull.* **24**, 42 (1999)
- [8] S. Schneider, *J. Phys. Cond. Matter* **13**, 7723 (2001)
- [9] S. Sastry, and C. A. Angell, *Nature Materials* **2**, 739 (2003)
- [10] P. R. ten Wolde, and D. Frenkel, *Science* **277**, 1975 (1997)
- [11] V. Talanquer, and D. W. Oxtoby, *J. Chem. Phys.* **109**, 223 (1998)
- [12] F. Sciortino, *J. Phys. Cond. Matter* **17**, v7 (2005)
- [13] X. Limei, S. V. Buldyrev, C. A. Angell, and H. E. Stanley, *Phys. Rev. E* **74**, 031108 (2006)
- [14] X. Limei, S. V. Buldyrev, N. Giovannibattista, C. A. Angell, and H. E. Stanley, *J. Chem. Phys* **130**, 054505 (2009)
- [15] J. P. K. Doye, D. J. Wales, F. Zetterling, and M. Dzugutov, *J. Chem. Phys.* **118**, 2792 (2003)
- [16] J. A. Moriarty, and M. Widom, *Phys. Rev. B* **56**, 7905 (1997)
- [17] N. W. Ashcroft, and N. D. Mermin, *Solid State Physics, Harcourt Brace & Co* (1976)
- [18] J.-P. Hansen, and I. R. McDonald, *Theory of simple liquids, Academic Press* (2006)
- [19] J.-F. Sadoc, and R. Mosseri, *Geometrical frustration, Cambridge University Press* (1999).
- [20] E. G. Ponyatovsky, *J. Phys. Cond. Matter* **15**, 6123 (2003)

- [21] I. Saika-Voivod, F. Sciortino, and P. H. Poole, *Phys. Rev. E.* **69**, 041503 (2004)
- [22] F. Sciortino, P. Tartaglia, and E. Zaccarelli, *J. Phys. Chem.* **109**, 21942 (2005)
- [23] M. Elenius, and M. Dzugutov, *J. Phys. Chem.* **131**, 104502 (2009)
- [24] C. M. Dobson, *Nature* **426**, 884 (2003)
- [25] C. Way, P. Wadhwa, and R. Busch, *Acta Materialia* **55** (2007) 2977
- [26] We thank Prof. C. A. Angell for reading the manuscript, comments and discussions, and Prof. F. Sciortino for a discussion. We also thank the Centre for Parallel Computers (PDC) at the Royal Institute of Technology, Stockholm, and the Ekman Consortium for providing computer resources.

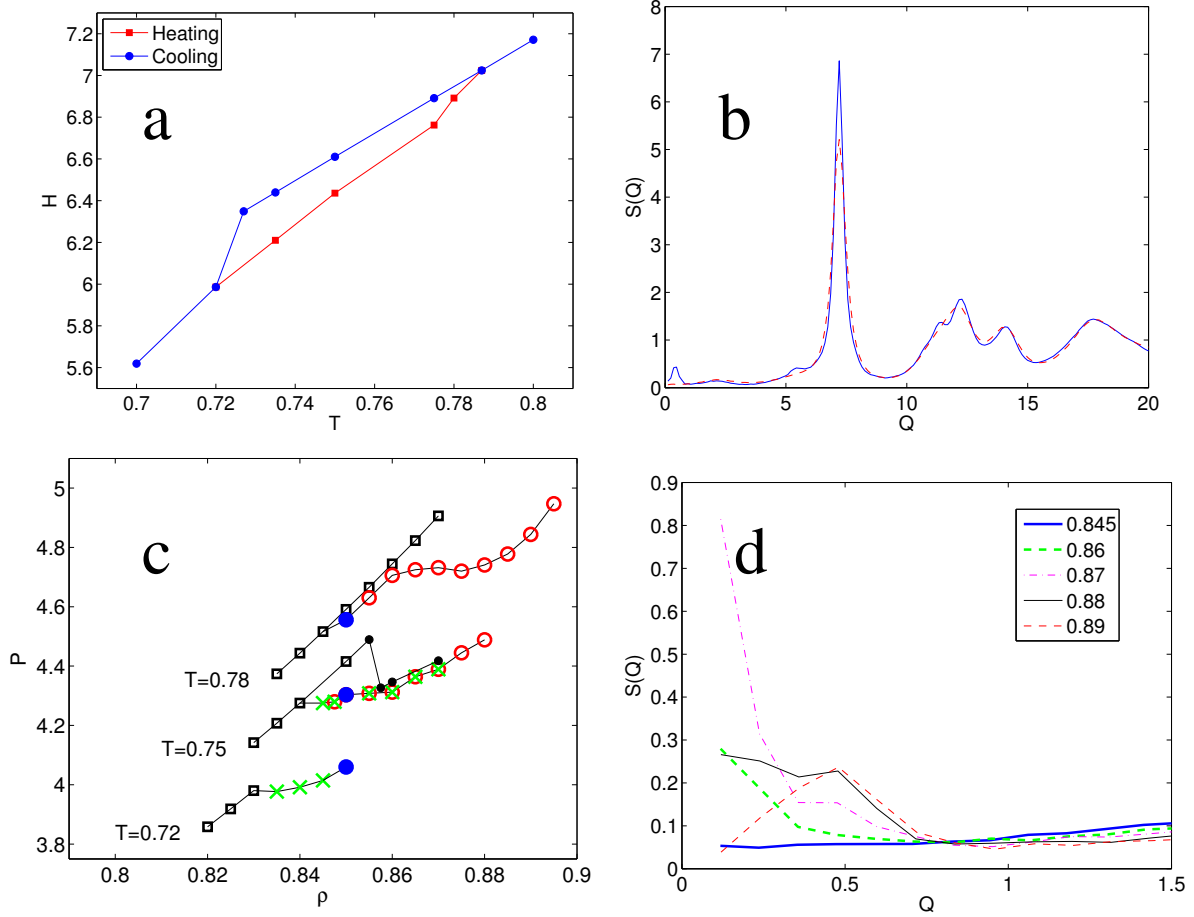


Figure 1: Liquid-liquid phase transition. The data represent a system of $N = 128000$ particles, unless indicated otherwise. **a.** Isochoric temperature variation of the enthalpy H at density $\rho = 0.85$. Circles, cooling; squares, heating. **b.** The structure factors $S(Q)$ of the HTL at $T = 0.78$ (dashed line) and LTL at $T = 0.68$ (solid line), both at the density $\rho = 0.85$. **c.** Isotherms crossing the region of the liquid-liquid transition. Open squares: HTL. Filled circles represent the $\rho = 0.85$ isochore shown in **a**. Open circles and crosses: LTL points obtained by isothermal compression and expansion, respectively. Small dots: LTL states simulated by the system of $N = 3456$ particles. The lines are included as a guide to the eye. **d.** Density variation of the low- Q behaviour of the structure factor along the $T = 0.78$ isotherm, for the indicated densities.

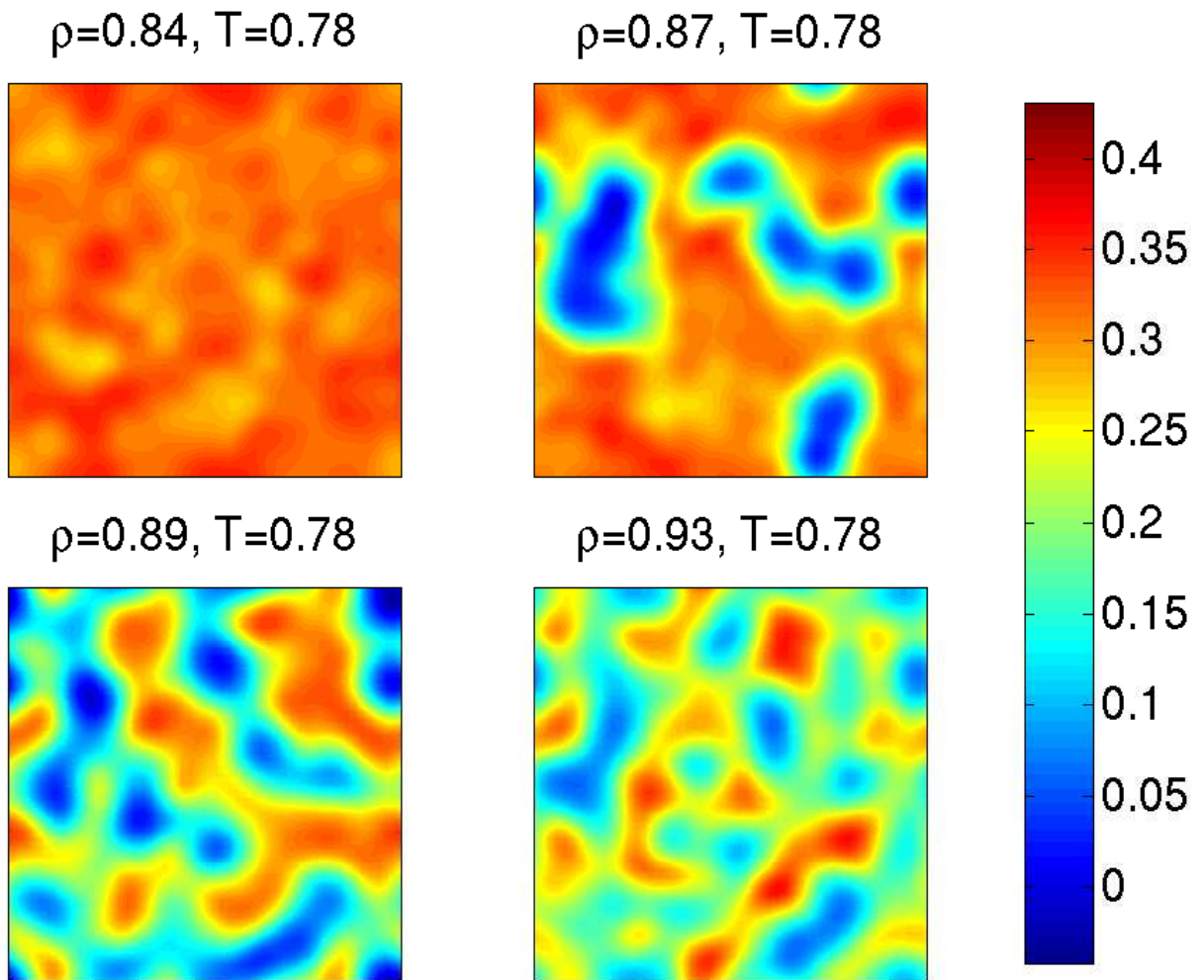


Figure 2: Cross-sections of the coarse-grained energy distribution in a system of 128000 particles at the thermodynamic states indicated in the plots. Each distribution has been averaged over 10^3 time steps.

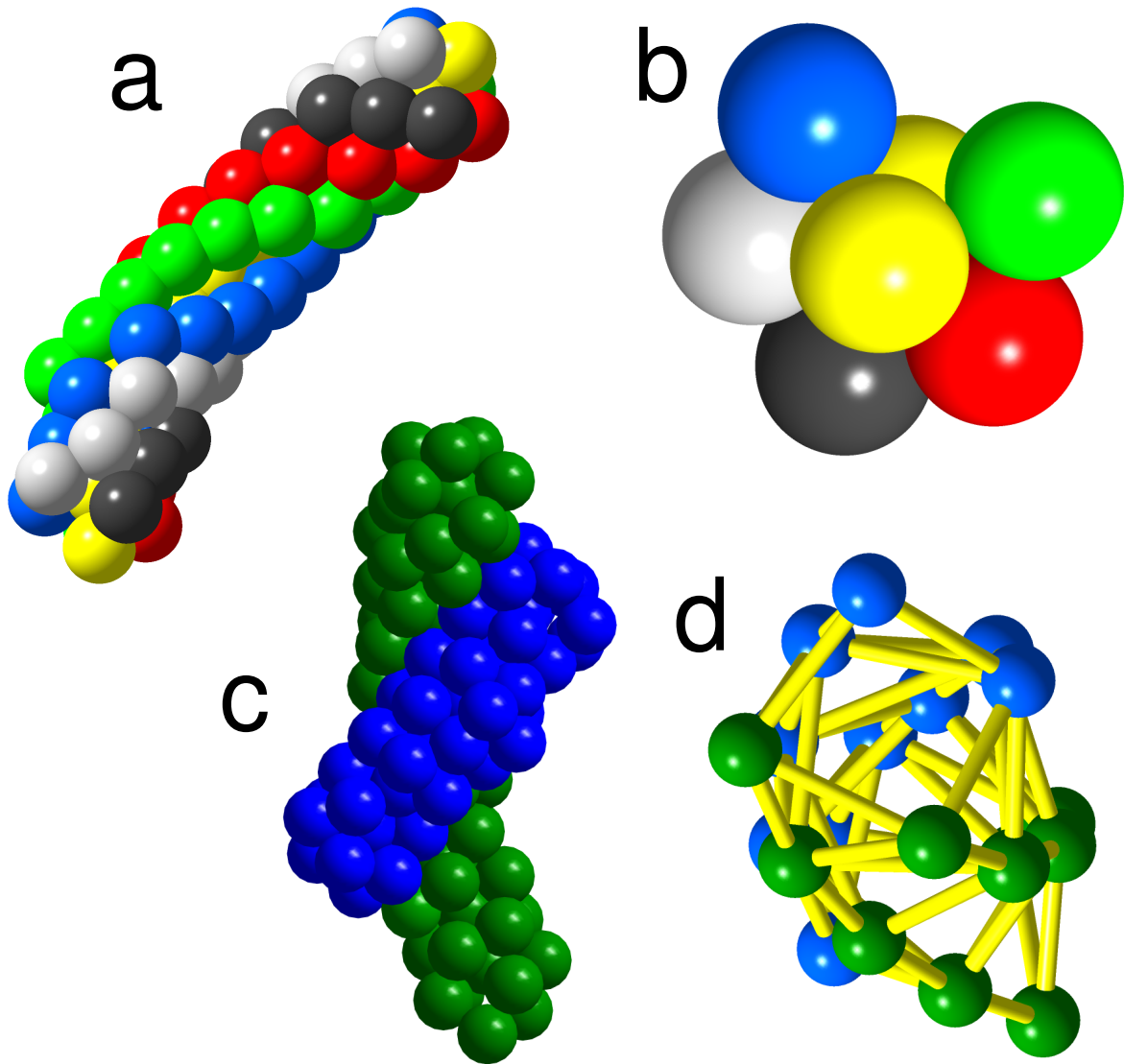


Figure 3: Structure of the LTL. **a**. A representative tetrahelical configuration discerned in a low-energy region observable in Fig. 2 for $\rho = 0.87$. The colors are a guide to the eye distinguishing the six constituent lines of atoms. **b**. A fragment of the configuration shown in **a** demonstrating a defect in pentagonal packing of tetrahedra. The colors are the same as in **a**. **c**. Aggregation of the tetrahelical cluster shown in **a** (green) with a similar cluster (blue). **d**. The linear strain of non-tetrahedral defects interfacing the two tetrahelical configurations is shown in **c** using the same colors. Atoms fulfilling the neighbor condition as described in the text are connected by bonds.

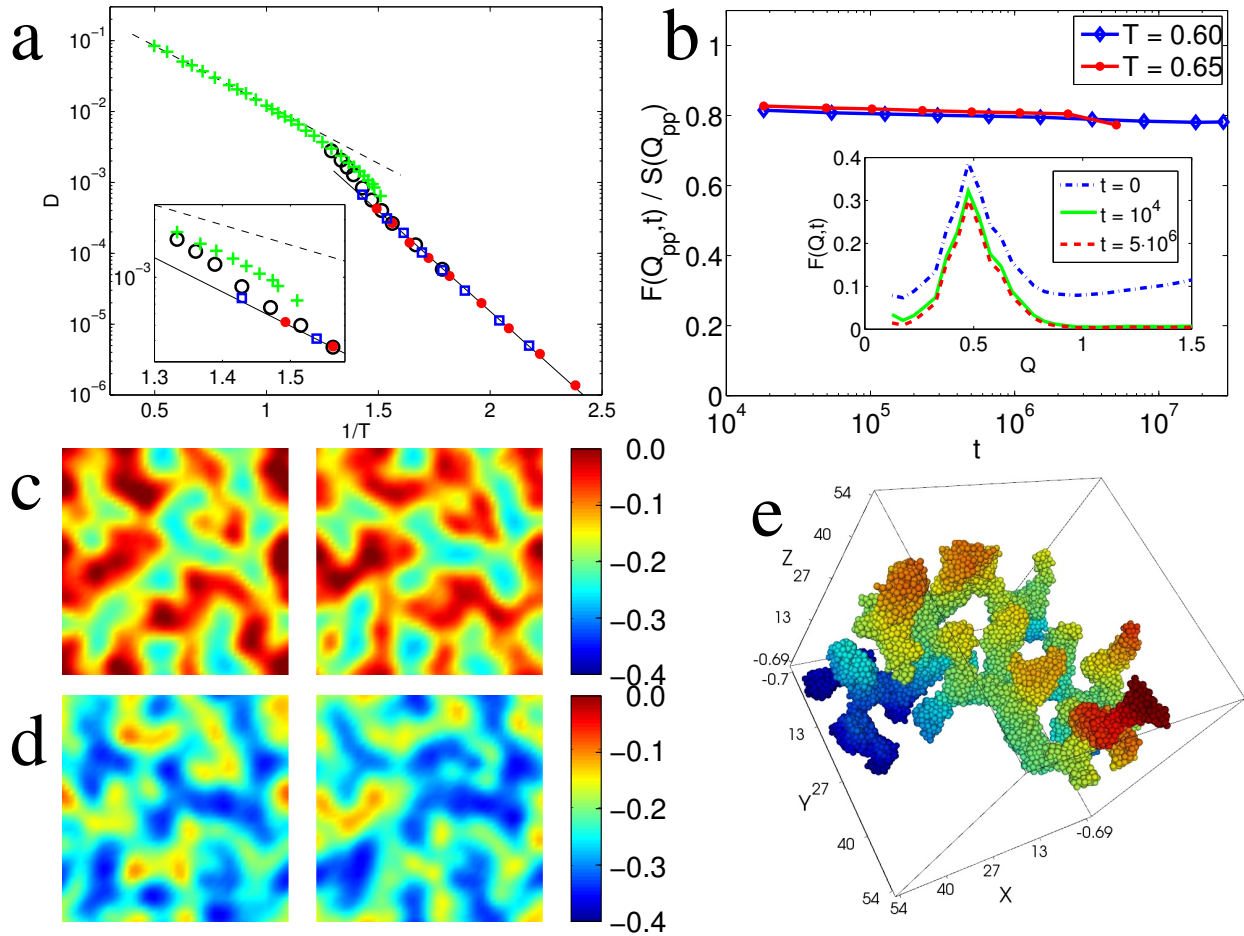


Figure 4: **a.** Arrhenius plot of the diffusivity at the density $\rho = 0.85$. Crosses, HTL (15). Open circles, LTL for the system of $N = 128000$. particles. Dots and open squares: LTL for the system of $N = 3456$ particles, under cooling and heating, respectively. The inset shows an enlargement of the transition area. The straight lines indicate Arrhenius fits to the data. **b.** Main panel: the intermediate scattering function $F(Q_{pp}, t)$, Q_{pp} being the position of the low- Q prepeak of $S(Q)$, for the LTL at $\rho = 0.85$ and the two indicated temperatures. Inset: the time evolution of $F(Q, t)$ in the small- Q domain. **c.** Two cross-sections of the coarse-grained energy distribution at $\rho = 0.85$ and $T = 0.65$ separated by the time interval of $0.5 \cdot 10^7$. **d.** The same as in **c** but for $T = 0.6$ and the separating time interval $3 \cdot 10^7$. **e.** A cluster composed of face-sharing tetrahedra detected within a low-energy domain of the configuration shown in **c**. The variation of color indicates the variation of Z -coordinate. The cluster includes 10456 atoms.